# Radius of Investigation for Reserve Estimation From Pressure Transient Well Tests

**Article** · January 2009

DOI: 10.2118/120515-MS



**1 author:**

Fikri Kuchuk
Schlumberger Limited
**237** PUBLICATIONS **1,280** CITATIONS

SEE PROFILE


SPE 120515

# Radius of Investigation for Reserve Estimation from Pressure Transient Well Tests

Fikri J. Kuchuk, SPE, Schlumberger



## Abstract

Although it is often used in pressure transient testing, radius of investigation still is an ambiguous concept, and there is no standard definition in the petroleum literature. The pressure diffusion corresponds to an instantaneous propagation of the pressure signal in the entire spatial domain when a flow rate or pressure pulse is applied to the sandface (beginning of a drawdown or injection) of a well. However, the initial pressure propagation is not diffusive but it propagates like a wave with a finite speed. If we have a pressure gauge at a distance $\mathbf{r}$, we will only start to detect a pressure change (drop or increase) after a few seconds or minutes even if we have a perfect pressure gauge with 0.0 psi resolution. After the initial propagation, pressure starts to diffuse or propagates as diffusion and we start to observe pressure change at a given space and time above the pressure gauge resolution and natural background noise, which could be as high as 0.1 psi. One of the constant background noises is the effect of tidal forces.

In this work, we present new formulae for radius of investigation in radial-cylindrical reservoirs and new techniques for general systems. The new formulation takes into account the production rate from the system, formation thickness, and gauge resolution. It is shown that the conventional radius of investigation formula (Earlougher, 1977) for radial-cylindrical systems, which is given as $r_{inv} = 0.029\sqrt{\frac{kt}{\phi\mu c_t}}$, yields very conservative estimates, and it could be as high as 30 to 50% lower. Radius of investigation is fundamental for understating of the tested volume; i.e., how much reservoir volume is investigated for a given duration of a transient test? For exploration wells, the reservoir volume investigated is one of the main objectives of running drillstem test (DST) or production tests. Therefore, how far pressure may diffuse (radius of investigation) during a transient test is very important for exploration well testing.

## Introduction

The challenge in estimating reserves from pressure transient well test data very often arises in oil and gas explorations as well as in other oil industry applications. Thus, determining radius of investigation during a pressure transient test becomes critically important. It may also be called transient drainage radius. Although it is often used in pressure transient testing, radius of investigation still is an ambiguous concept, and there is no standard definition in the petroleum literature. For instance, it is defined at http://www.glossary.oilfield.slb.com/ as the calculated maximum radius in a formation in which pressure has been affected during the flow period of a transient well test. This definition is not completely accurate when we apply an instantaneous source during which pressure may diffuse to a long distance. Therefore, to understand the radius of investigation, first we look at the pressure distributions in a 1D radial-cylindrical homogenous reservoir produced by a fully completed vertical well, in which after the wellbore storage effect the flow regime is predominantly radial before the effect of any outer boundary. Note that this may not be true for wells in nonhomogenous and heterogeneous formations and reservoirs. Nevertheless, understanding the fundamental radial flow regime is essential to interpreting pressure transient testing and its radius of investigation; *i.e.*, how much reservoir volume is investigated for a given duration of a transient test? For exploration wells, the reservoir volume investigated is one of the main objectives of running DST or production tests. Therefore, how far pressure may diffuse (radius of investigation) during a transient test is very important for exploration well testing where very important decisions are made based on total volume are seen by DST or other production tests.

Transient, pseudosteady-state and steady-state solutions for various bounded and unbounded reservoirs have been presented in the petroleum literature (Hurst, 1934; Muskat, 1934)) since 1930s. However, the idea of the radius of investigation (drainage radius) was set in motion by two seminal papers. The first paper by Miller et al. (1950) presented the time approach steady state, where a time to reach the steady-state condition from the transient period was given. This paper further stated that the time to reach the steady-state condition is independent of production rate and net thickness of the formation. The second paper by Horner (1951) presented a method for estimating the fault distance to well from buildup tests. Finally, Van Poolen (1964) presented the well-known radius of investigation or drainage radius formula as

$$r_{inv} = 0.029\sqrt{\frac{kt}{\phi\mu c_t}}. \tag{1}$$

Various authors have since presented slightly different constants from 0.029; thus Eq. 1 can be expressed as

$$r_{inv} = c_r\sqrt{0.0002637\frac{kt}{\phi\mu c_t}}, \tag{2}$$

where $c_r$ is given as 1.78 (this gives the constant 0.029 given in Eq. 1) by Van Poolen (1964). Table 1 presents various values of $c_r$ from different investigators (modified from Daungkaew et al. 2000). Recently, Stewart (2007) also presented another formula for the radius of investigation for buildup tests as

$$r_{inv} = 0.171\sqrt{\frac{qt}{\delta ph\phi c_t}}, \tag{3}$$

where $\delta p$ must be greater than the pressure gauge resolution. It should be noted that this radius of investigation formula is independent of permeability and viscosity.

**Table 1-Comparison of $c_r$**

| Author | $c_r$ |
|---|---|
| Brownscombe and Kern (1951) | 1.783 |
| Chatas (1953) (linear flow) | 1.41 |
| Daungkaew et al. (2000) | 0.379-1.623 |
| Finjord (1988) | 2.82 |
| Hurst (1961) | 2.8284 |
| Hurst et al. (1969) | 2.64 |
| Johnson (1988) | 2.81 |
| Jones (1962) | 4 |
| Kutasov and Hejri (1984) | 2.03-2.14 |
| Lee (1982) | 2 |
| Muskat (1937) | 2 |
| Streltsova (1988) | 2 |
| Tek et al. (1957) | 4.29 |
| Van Poolen (1964) | 2 |
| Van Poolen (1964) | 1.78 |

## Pressure Propagation and Diffusion in Infinite Porous Media

The flow of a slightly compressible fluid with a constant compressibility ($c_t$) and viscosity ($\mu$), the pressure diffusion in an isotropic homogenous porous medium is governed by the pressure diffusion equation that can be written as

$$\frac{k}{\mu}\nabla^2 p(\mathbf{r},t) = \varphi\frac{\partial p(\mathbf{r},t)}{\partial t}, \tag{4}$$

where $\varphi = \phi c_t$. As pointed out by Morse and Feshback (1953), the pressure diffusion given by Eq. 4 implies that the pressure in the fluid-filled porous medium due to a pressure or rate pulse in a well will change (drop or rise depending on whether it is a source/sink) instantaneously everywhere in the medium although not at the same rate. Furthermore it implies that the speed of pressure diffusion is infinite. This is an impossibility because Einstein's theory of relativity

states that nothing can travel faster than the speed of light. Thus, a local excitation (source/sink) in a porous medium should not be instantaneously felt throughout the medium. It takes time for a pressure disturbance to propagate from its source to other positions in the medium due to the finite speed of sound and signal propagations. Foster et al. (1967) showed that including the initial sound propagation (neglecting signal propagation) due to a source-sink excitation leads to the telegraphers equation for a compressible Newtonian fluid in an isotropic (can also be easily extended for anisotropic and heterogeneous systems) rigid porous medium and given as

$$\frac{k}{\mu}\nabla^2 p(\mathbf{r},t) = \varphi\frac{\partial p(\mathbf{r},t)}{\partial t} + \frac{k}{\mu}\frac{1}{v_{as}}\frac{\partial^2 p(\mathbf{r},t)}{\partial t^2}, \tag{5}$$

where $v_{as}$ is the isothermal speed of sound in liquid-filled porous media; about 343 m/s in the air at atmospheric conditions and about 1,500 m/s in sea water. In the gas, oil, and water-filled porous medium, it varies a few hundred to 1,000 m/s. Therefore, as also pointed out by Foster et al. (1967) andJohnson (1988), the radius of investigation for the pressure propagation is given as

$$r_{inv} = v_{as}t, \tag{6}$$

where $t$ is measured from the starting time of the source-sink excitation. As can be seen from Eq. 5, the pressure signal will propagate about 1,000 m in 1 second in a light oil-filled porous medium. This is the only definable radius of investigation, and Eqs. 4 and 5 do not imply any other radius of investigation for fluid flow in porous media. Then the question becomes, is this observable? For instance, at high frequencies, say 300 kHz, it is observable, but at low frequencies in pressure transient tests, where frequencies are less than 1 Hz, the pressure disturbance due to the sound and signal propagations is not observable anywhere in the system with the current testing measurement technologies. Therefore, the sound propagation term in Eq. 5 becomes negligible in a short time, within a few seconds, and then the pressure transient becomes totally diffusive and is governed by Eq. 4.

From now on when we refer the radius of investigation, we mean that when the pressure change becomes observable at a given a spatial coordinate and time, we substitute the spatial coordinate with *radius of investigation*. The notion of what is observable then becomes dependent on detection instruments or pressure gauges in pressure diffusion. When the pressure change becomes observable, it has to be *measurable and quantifiable*.

It would have been relatively easy to determine an observable radius of investigation if we have distributed pressure sensors throughout the reservoir. For instance, Fig. 1 presents the pressure response in an observation well. Because we know the location of the observation well (the radius of investigation), what we are observing is the time the pressure diffusion becomes observable but this is not the arrival of the signal in terms of the pressure propagation and diffusion; *i.e.*when the change in pressure becomes observable from the background pressure. It is about 36.25 hr. At this scale, which is about 1 psi per division, the background pressure appears perfectly smooth.

Figure 2 presents a portion of the same data where the plot is expanded to 0.001 psi per division around the start of observable pressure change. The pressure looks noisy and it almost randomly varies within 0.01 psi from 35 to 36 hr. In fact 0.004 psi was the stated resolution of the quartz gauge used for this test. Although it will not have any significant effect, the change in pressure observable from the background pressure could be at any time from 36.00 and 36.30 hr (uncertainty interval).

To make this point clear, let us give another example. Suppose that a homogeneous reservoir with a fully penetrated vertical well is cut through a sealing (no-flow) fault. Using the method of images, the well- known solution for the pressure distribution in the system with a single sealing fault located at a distance $d$ can be written as

$$p_D(r_D,t_D) = \frac{1}{2}\left[\mathrm{E}_1\left(\frac{r_D^2}{4t_D}\right) + \mathrm{E}_1\left(\frac{r_d^2}{4t_D}\right)\right], \tag{7}$$

where the dimensionless time and pressure (in field units) are $t_D = \frac{0.0002637kt}{\pi\phi\mu c_t r_w^2}$ and $p_D = \frac{kh}{141.2q\mu}[p_o - (p_w)(t)]$, $r_D = r/r_w$, and $r_d = 2d/r_w$ is the dimensionless distance.

Given the fault distance, when is the effect of the fault felt at the wellbore? In other words, when will the wellbore pressure deviate from the infinite-acting solution (the first term in Eq. 7). The additional pressure increase due to a sealing fault is given by the second term in Eq. 7 and plotted in Fig. 3 for $r_w$= 0.35 ft, $d$ = 700 ft, production rate, $q$ = 1,000 B/D, and other reservoir parameters given in Table 2. The pressure increase due to the fault will be felt at the wellbore just after the pressure propagation that may last less than a few seconds as stated previously (Fig. 3). The question is at what time the pressure increase becomes observable at the wellbore. As can be seen in

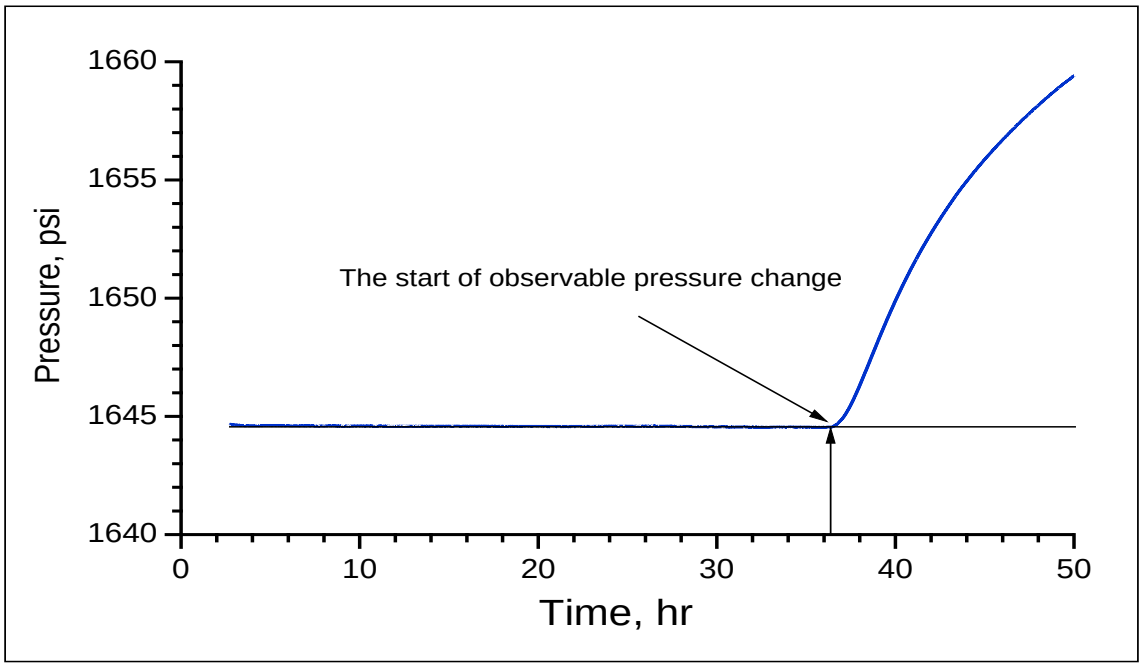


**Fig. 1—Pressures response at an observation well due to an injector.**

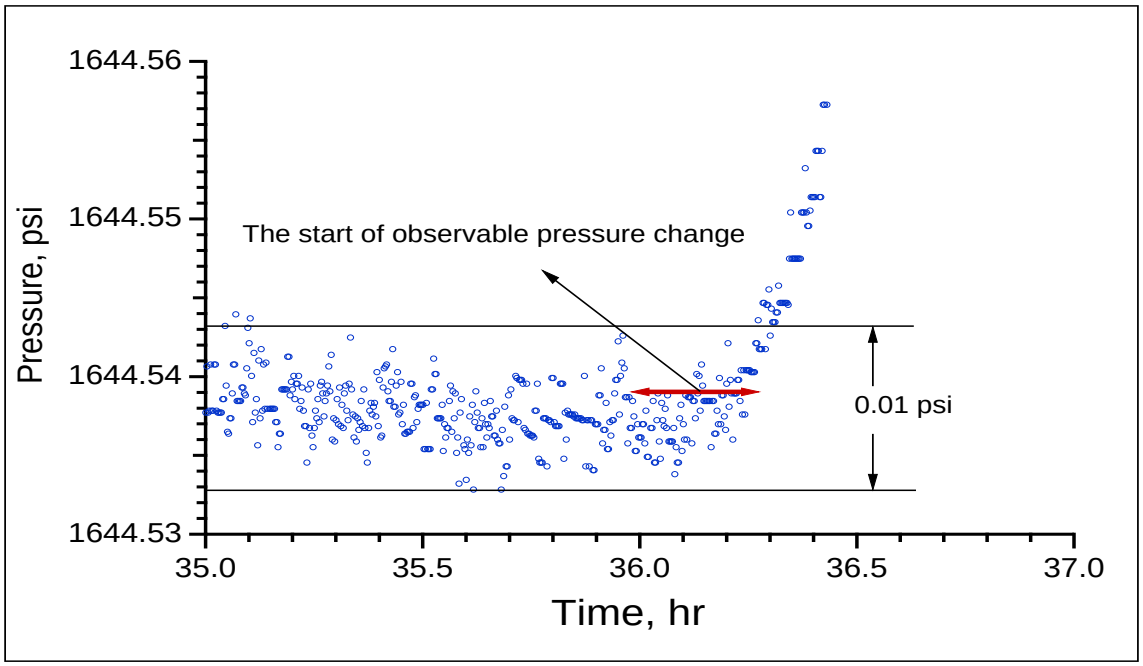


**Fig. 2—Pressures response at an observation well due to for an injector.**

| Table 1-Formation and fluid properties | | | | |
|---|---|---|---|---|
| $h$ (ft) | $k$ (md) | $\phi$ | $\mu$ (cp) | $c_t$ (psi$^{-1}$) |
| 100 | 100 | 0.2 | 1.0 | $10^{-5}$ |

Figure 3, it depends on the gauge resolution. If the resolution is 0.00001 psi, it is impossible to attain with the current pressure gauges, the pressure increase becomes observable at 3.4 hr. If the resolution is 0.01 psi, the pressure increase becomes observable at 7.7 hr. The pressure increase becomes observable at 12.7 hr for a 0.1− psi resolution and 29.5 hr for a 1− psi resolution, and so on. In reality the background noise will reduced the effective gauge resolution. The production noise in the wellbore is a well-known phenomenon particularly during drawdown/injection tests. This is why buildup and interference tests are preferred for observing boundary effects. As also can be clearly seen in Fig. 3, when the flow rate is reduced from 1,000 to 200 B/D, it takes longer for the pressure increase to be observable at the wellbore. For instance, the pressure increase becomes observable at 10.6 hr for a 0.01− psi resolution, and 21.1 hr for a 0.1− psi resolution, and 94.5 hr for a 1− psi resolution. These curves clearly show that there is no abrupt change in the pressure behavior due to a sealing fault at 700 ft; both pressure and its derivative are continuous.

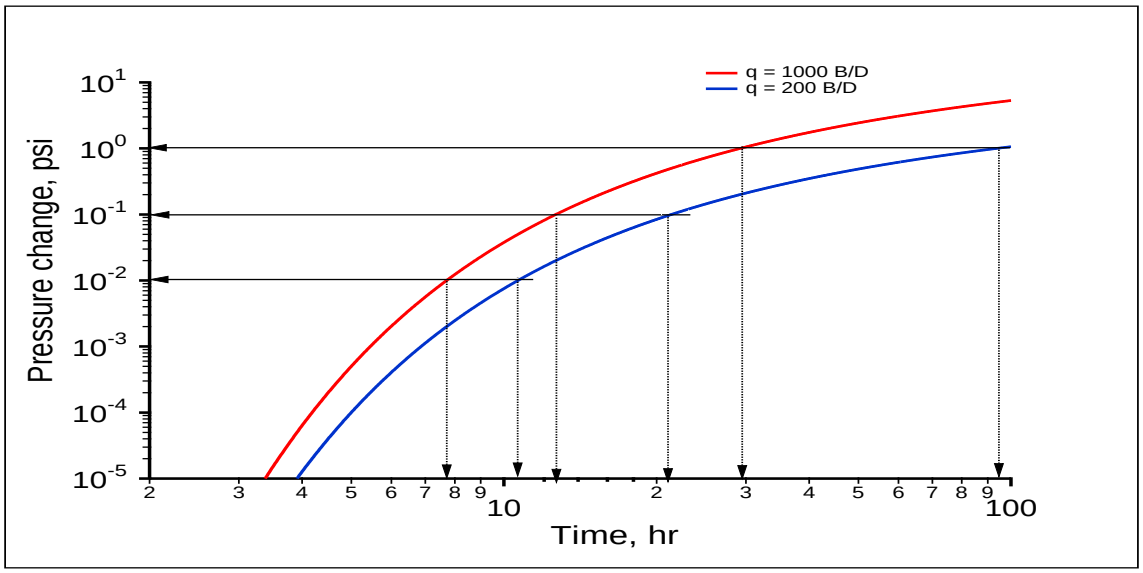


**Fig. 3—Additional pressures changes at the wellbore due to a sealing fault.**

Figure 4 presents the same data given in Figure 3 in a linear plot. This linear plot of the data gives an impression that we have a definite pressure diffusion arrival time as in Fig. 1. This is just a visual illusion without observable and measurable quantification.

Figure 5 presents derivatives corresponding to the infinite-acting system and the sealing fault model given by Eq. 7 and for the same reservoir parameters ($q = 1,000$ B/D, etc.). As can be seen in this figure, there are three distinct flow regimes for the fault model that are observed:

1. The infinite-acting period before 7.4 hr during which the derivatives of two systems are indistinguishable at this scale *i.e.*, the difference in the derivatives of two systems is not observable at the scale of Fig. 5. Of course, as we observed in Fig. 3, the difference of the wellbore pressures of the two systems is about 0.01 psi at 7.4 hr.

2. The transition region lasts more than two log cycles from 7.4 to 2,300 hr.

3. The second infinite-acting flow regime is due to the semi-infinite system. The semilog slope of the system becomes twice of that from the first infinite-acting period.

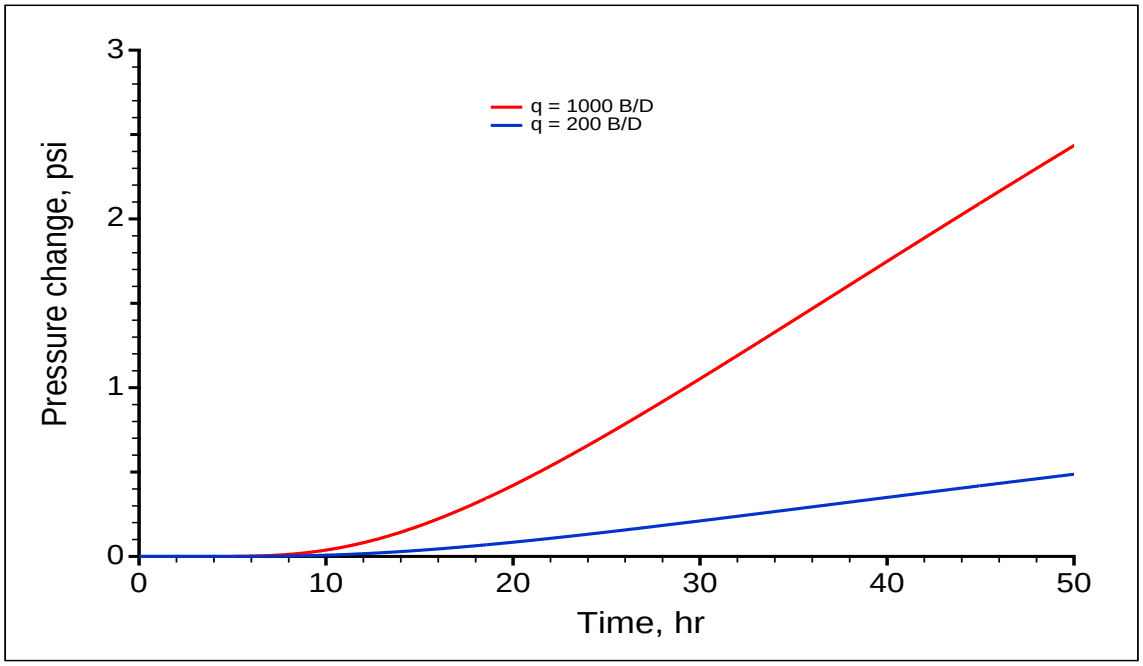


**Fig. 4—Additional pressures changes at the wellbore due to a sealing fault.**

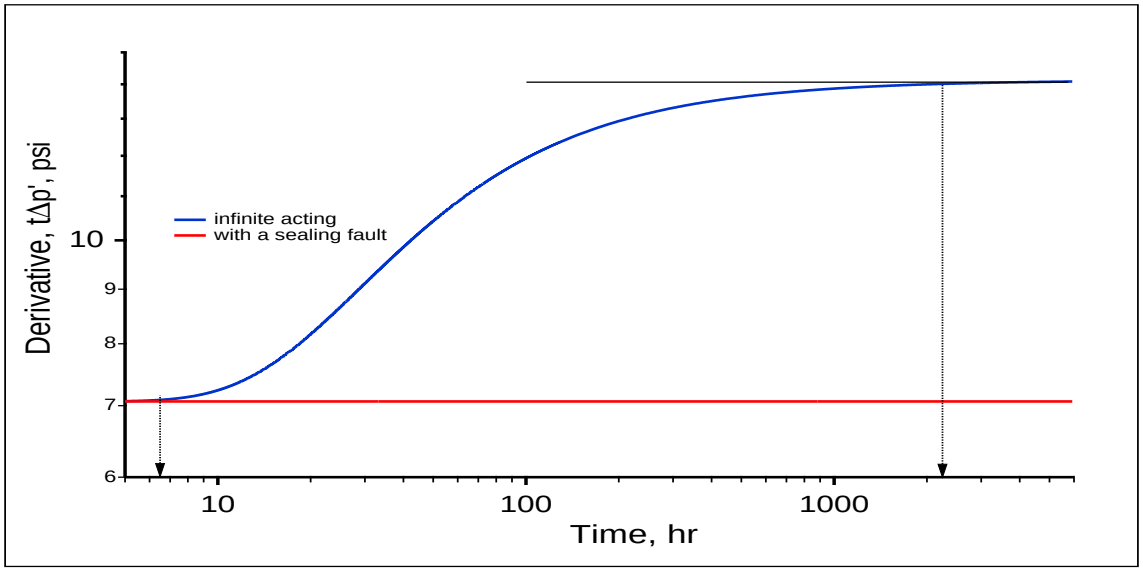


**Fig. 5—Derivatives of the wellbore pressures for an infinite-acting system and a reservoir with a sealing fault.**

The next question is what should the constant $c_r$ be in Eq. 2 that satisfies the observable separation of two derivatives at 7.4 hr? It is $c_r = 2.2397$, which is 20% higher than 1.78 of the conventional formula. The fault distance from the conventional formula given by Eq. 1 is estimated to be 556 ft, which is 20% lower than the actual value of 700 ft. It should be emphasized that this is at which time the effect of a sealing fault becomes observable if we have a pressure gauge with a $0.01-$ psi apparent resolution in the wellbore. The apparent resolution should be defined as the gauge resolution plus the natural background noise; *i.e.*, it is the resolution at which a pressure gauge starts measuring an observable pressure change due to a flow rate pulse in a reservoir or wellbore, where the pressure is constant or stable everywhere and the natural background noise does not have very high-frequency components. For instance, pressure measurements have a significant level of high-frequency noise in a producing wellbore. Except during the initial period of shut-in, high frequency noises almost disappear during middle and late time periods of a buildup test. We cannot estimate a radius of investigation for this reservoir with a fault for the times larger than the time at which the effect of a sealing fault becomes observable because the pressure distribution about the origin will not be symmetric anymore. This will be discussed later.

Now let us examine a totally bounded closed reservoir (also called no-flow outer boundary) for which transient and pseudosteady-state solutions have been presented in the petroleum literature (Hurst, 1934; Muskat, 1934, 1937; van Everdingen and Hurst, 1949) since 1930s. The dimensionless pressure distribution in the Laplace domain for a fully penetrated well producing at a constant rate in the center of a closed circular reservoir is given as (van Everdingen and Hurst, 1949)

$$\bar{p}_D(r_D, s) = \frac{1}{s\sqrt{s}} \frac{\mathrm{K_0(r_D\sqrt{s})\, I_1(r_{eD}\sqrt{s}) + I_0(r_D\sqrt{s})\, K_1(r_{eD}\sqrt{s})}}{[\mathrm{K_1(\sqrt{s})\, I_1(r_{eD}\sqrt{s}) - I_1(\sqrt{s})\, K_1(r_{eD}\sqrt{s})}]}, \tag{8}$$

where $r_D = r/r_w$, $r_{eD} = r_e/r_w$, $r_e$ and $r_w$ are the external radius of the closed circle and wellbore radius, respectively. The Laplace domain variable $s$ corresponds to $t_D$. When $t_{DA} \geq 0.1$ (Ramey and Cobb, 1971), the system reaches the pseudosteady-state condition due to the no-flow boundary, the solution given by Eq. 8 can be written at the wellbore as

$$p_D(t_{DA}) = 2\pi t_{DA} + \frac{1}{2}\ln(A) - 1.322364, \tag{9}$$

where the dimensionless time based on the drainage area ($A$) is defined as $t_{DA} = t_D \frac{r_w^2}{\pi r_e^2}$.

Although the van Everdingen and Hurst (1949) solution is correct, but the dimensionless pressures given for large $t_D$ and $r_{eD}$ are slightly incorrect (numbers are still remarkable given the computing power in 1949). For instance, Table 3 presents dimensionless pressures given in Table IV of van Everdingen and Hurst (1949) for $r_{eD} = 2000$, and computed from Eq. 8. As can be observed from this table, the error at $t_D = 400,000$ is 0.003% and becomes 24% at $t_D = 6,400,000$. After reaching the pseudosteady-state condition, the dimensionless pressures computed from Eq. 8 and Eq. 9 become almost identical.

**Table 2-Comparison of Solutions**

| $t_D$ | $p_{eD-veh}$ | Eq. 8 | Eq. 9 |
|---|---|---|---|
| 400000 | 6.854 | 6.8542 | 7.0509 |
| 600000 | 7.056 | 7.0578 | 7.1509 |
| 1000000 | 7.298 | 7.3295 | 7.3509 |
| 4000000 | 7.597 | 8.8505 | 8.8509 |
| 6000000 | 7.601 | 9.8483 | 9.8509 |
| 6400000 | 7.601 | 10.0532 | 10.0509 |

Without losing any accuracy, Eq. 8 can also be written at the wellbore ($r_D = 1$) as

$$\bar{p}_D(r_D, s) = \frac{1}{s}\left[\frac{\mathrm{K_0(\sqrt{s})}}{\sqrt{s}\mathrm{K_1(\sqrt{s})}} + \frac{\mathrm{I_0(\sqrt{s})\, K_1(r_{eD}\sqrt{s})}}{\mathrm{I_1(r_{eD}\sqrt{s})}}\right]. \tag{10}$$

It is very clear from this equation that the first term in Eq. 10 is the infinite acting part (the cylindrical-source solution in an infinite system ) of the solution and the second term is due to the outer boundary. The additional pressure increase due to a no-flow closed boundary is given by the second term in Eq. 10 and plotted in Fig. 6 for

$r_w$= 0.35 ft, $r_e$ = 700 ft, production rate, $q$ = 1,000 $B/D$, and other reservoir parameters given in Table 2. The pressure increase due to the no-flow boundary will be felt at the wellbore just after the pressure propagation. As can be seen from Fig. 6, the pressure increase becomes observable in the wellbore at 5.4 hr if the resolution is 0.01 psi, 7.8 hr for 0.1 psi, and 13.3 hr for 1 psi. For a production rate of 200 B/D, they are 6.9, 11, and 23.6 hr for 0.01, 0.1, and 1 psi resolutions, respectively. As in the sealing fault case, these curves clearly show that there is no abrupt change in the pressure due to a no-flow boundary at 700 ft.

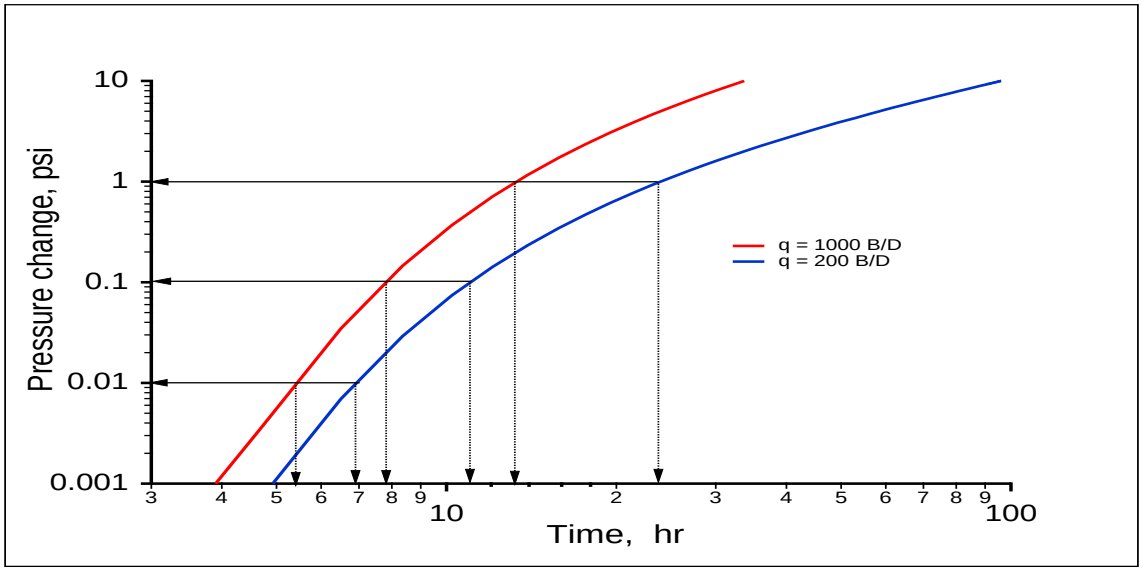


**Fig. 6—Additional pressures change at the wellbore in a closed no-flow reservoir.**

Figure 7 presents derivatives corresponding to the infinite-acting system and a closed circular reservoir Eq. 8 (the same parameters as in Fig. 6) As in the sealing fault case, there are three distinct flow regimes (Fig. 7 ) that are observed:

1. The infinite-acting period before 5.4 hr during which the derivatives of two systems are indistinguishable at the scale of this figure. It was 7.4 hr for the sealing-fault model because the pressure declines much faster in a close system than that is for a semi-infinite system. Of course, as we observed in Fig. 6, the difference of the wellbore pressures of the two systems is about 0.01 psi at 6.9 hr and 0.1 psi at 11 hr.

2. The transition region that lasts less than a half-log cycle; *i.e.*from 5.4 to 16 hr (more than two log cycles for the sealing-fault model).

3. The pseudosteady-state flow regime that starts at 16 hr and is characterized by a positive unit slope on the derivative plot.

For this case, the constant $c_r$ in Eq. 2 that satisfies the observable separation of two derivatives at5.4 hr is 2.622, which is 32% higher than 1.78 of the conventional formula. $c_r$ would be 1.60 if we use the start of the pseudosteady-state flow regime at 16 hr. The radius of investigation from the conventional formula (that is computed from the start pseudosteady-state flow regime) given by Eq. 1 is estimated 817 ft, which is 17% higher than the actual value of 700 ft and the reserve will be 36% higher.

It should be stated again that when the system reaches the pseudosteady-state condition due to a no-flow boundary at $t_{DA} = 0.1$, at which the approximation given by Eq. 9 becomes applicable, this $t_{DA}$ of 0.1 has nothing to do with the radius of investigation or observable radius of investigation. This is the time at which a closed system reaches the pseudosteady-state condition. As can be observed in Fig. 6, the difference in the wellbore pressures of the two systems at 16 hr, at which the pseudosteady-state condition attained in the reservoir, is about 1 psi.

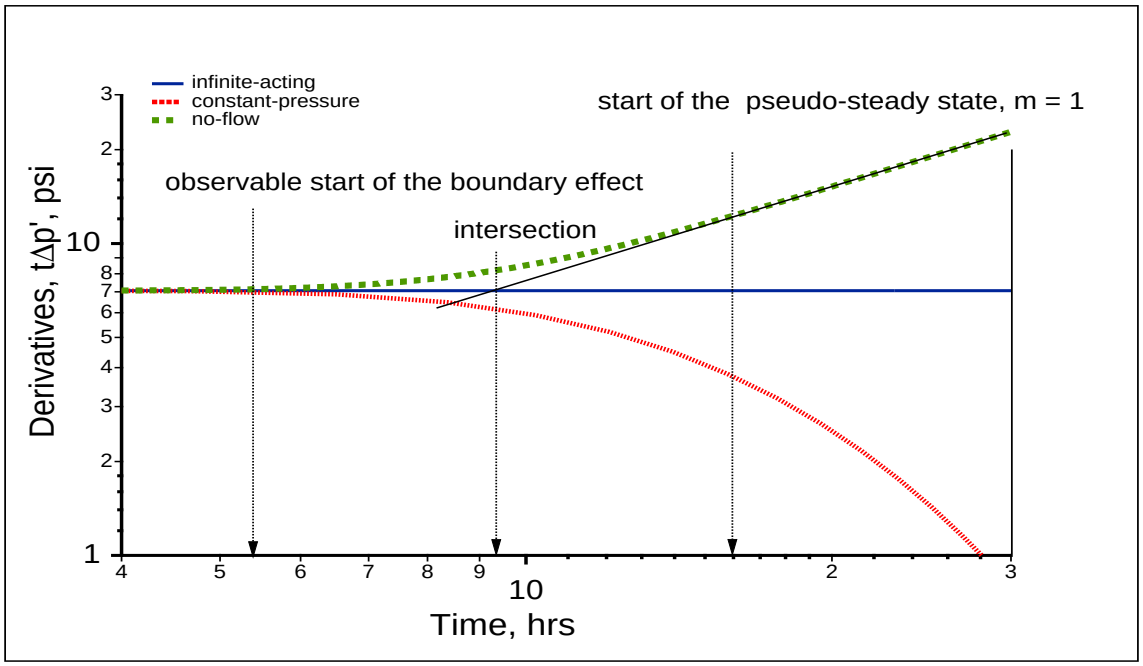


**Fig. 7—Derivatives of the wellbore pressures for an infinite-acting system, and a no-flow and constant-pressure outer boundary systems.**

## Radius of Investigation

Recently, Whittle and Gringarten (2008) suggested using the intersection as shown in Fig. 7 for calculating the radius of investigation from derivative curve. From the logarithmic derivative of $p_D(t_{DA})$ given by Eq. 9, the dimensionless (based on the drainage area) intersection time $t_{DA}$, where $p_D t_{DA} = 0.5$ (the infinite-acting slope as shown in Fig. 8), can be written as

$$t_{DA} = \frac{1}{4\pi} = \frac{0.0002637kt}{\pi\phi\mu c_t \pi r_e^2}, \tag{11}$$

from which a radius of investigation formula can be written as

$$r_{inv} = 2\sqrt{0.0002637\frac{kt_{int}}{\phi\mu c_t}} = 0.03248\sqrt{\frac{kt_{int}}{\phi\mu c_t}} \tag{12}$$

or given by Whittle and Gringarten (2008) as

$$r_{inv} = 0.2729\sqrt{\frac{qt_{int}}{h\phi\mu c_t \Delta\acute{p}_{int}}}, \tag{13}$$

where $t_{int}$ is the time at which the pseudosteady-state flow unit slope intersects the infinite-acting line (zero slope) and $\Delta\acute{p}_{int}$ is the value of the derivative of the infinite acting period. These radii of investigation formulae given by Eqs. 12 and 13 are identical. It should be stated that these are really not radius of investigation formulae. They yield the radius of a closed-boundary reservoir at which the system reaches the pseudosteady-state condition. In other words, when the pseudosteady-state flow regime (a unit slope on the log-log derivative plot) these radii of investigation formulae yield the radius of a closed circular reservoir. It should not be used for determining radius of investigation for any other systems, including infinite and semi-infinite reservoirs.

Using values from Fig. 7 and Eqs. 12 or 13, $r_{inv}$ is estimated 703 ft, which is almost exact (700 ft input value). Both formulae given above work remarkably well for calculating the radius of a closed circular-boundary reservoir. Should these formulae be used at the start pseudosteady-state flow regime, where the unit slope is not apparent? For instance, should they be used for a constant-pressure outer boundary reservoir as shown in Fig. 7, where we

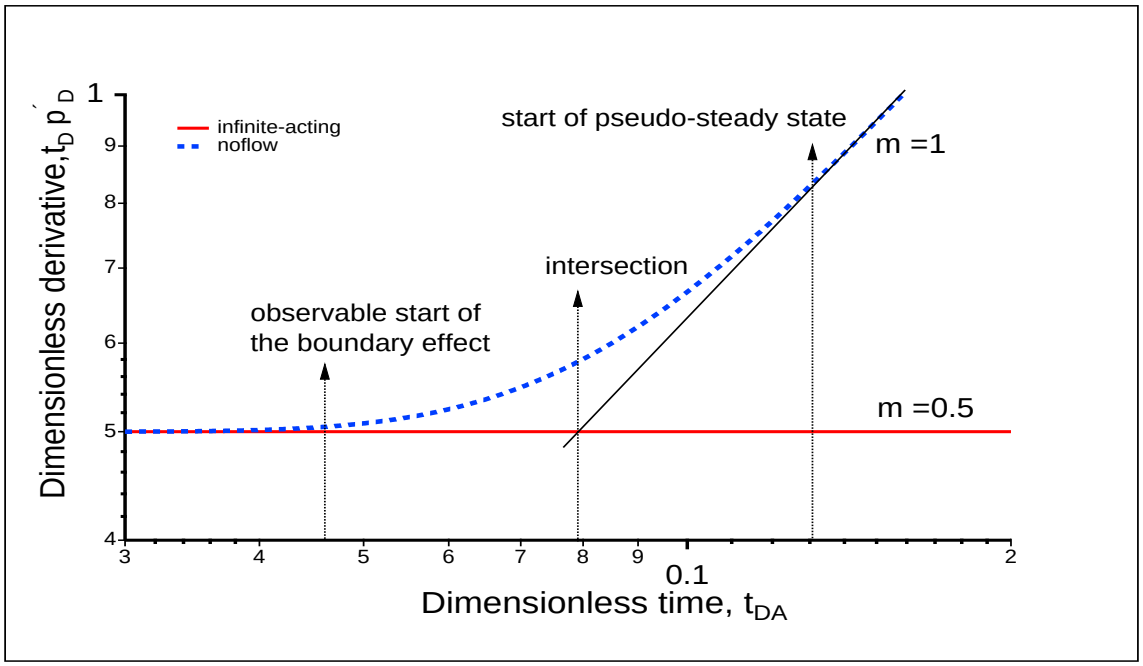


**Fig. 8—Dimensionless pressure derivatives for infinite-acting and no-flow outer boundary systems as a function of dimensionless time $t_{DA}$.**

do not have any intersection but an apparent deviation time from the infinite-acting line (zero slope) as in the sealing fault example given above? If we were to use 5.4 hr (the observable deviation time of constant-pressure outer boundary case from the infinite-acting line as shown in Fig. 7), the radius of investigation from the conventional formula given by Eq. 1 is estimated 475 ft, which is 32% less than the actual value of 700 ft and 534 ft from Eq. 12, which is 24%. The estimated reserve from these radii of investigation will be 54% and 42% lower respectively. As we said above except for fully no-flow closed systems, for many reservoirs such as infinite-acting, partially closed (no flow), constant-pressure boundary including systems with fault, fractures, etc., radii of investigation formulae given by Eqs. 1, 12, and 13 should not be used.

Following Hurst (1961), we can also use the time, $t_{DA} = 0.046$ as shown in Fig. 8, at which the separation of two derivatives becomes observable (at the scale of the plot, if the scale is expanded then the time becomes smaller) as shown in Fig. 7, for calculating the radius of investigation, which yields

$$r_{inv} = 2.631\sqrt{0.0002637\frac{kt_{st}}{\phi\mu c_t}} = 0.04272\sqrt{\frac{kt_{st}}{\phi\mu c_t}} \tag{14}$$

where $t_{st}$ is the time at which the deviation of the pressure derivatives of the no-flow or the constant- pressure boundary systems from the infinite-acting line (zero slope) becomes observable.

Using Eq. 14 and $t_{st} = 5.4$ hr from Fig. 7, the radius of investigation is estimated to be 702 ft, which is almost exact. As shown in Fig. 6, the additional pressure drop due to the no-flow boundary is 0.01 psi at $t_{st}$=5.4 hr. Unlike Eqs. 12 and 13, Eq. 14 will also work for the constant-pressure outer boundary case as shown in Fig. 7.

Using Eq. 14 and $t_{st} = 7.4$ hr from Fig. 5, the distance to the fault is estimated to be 818 ft, which is 12% higher than the actual value. Nevertheless, the 12% difference is very small compared to the distance computed from Eqs. 1, 12, and 13. As shown in Fig. 6, the additional pressure drop due to the no-flow boundary is 0.01 psi at $t_{st} = 7.4$ hr.

Of course, using the same techniques we can also derive radius of investigation formulae for many different flow and reservoir geometries (hydraulically fractured wells, faulted, fractured, channel systems, etc.), and they will be more precise than those obtained from Eqs. 1, 12, 13, and 14 However, none of them should be used after the boundary effects become observable.

Thus far, we have presented synthetic data from well-defined analytical solutions with at least 4- to 6-digits accuracy. The best downhole pressure gauge resolution currently available is about 0.002 psi, and more common

gauges used in pressure transient tests have 0.01 psi resolution. Furthermore, as discussed above, the apparent resolution could be less than the stated gauge resolution in the wellbore. Therefore, noise is added to pressures that are computed from Eq. 8 with the same parameters as in Fig. 6 and production rate, $q = 1,000$ B/D. Two levels of noises are considered: 1) $\pm 0.1$ and 1) $\pm 0.01$ Gaussian distribution. A 0.01-hr-time window length is used for derivative smoothing. The actual derivative without noise is shown in Fig. 7. As can be seen from Fig. 9, the $\pm 0.01$ noise level did not significantly affect the start times of the observable boundary effect, intersection, and pseudosteady-state flow regime. On the other hand, the $\pm 0.1$ noise level did have a significant affect on the start times of the observable boundary effect, and pseudosteady-state flow regime, but not the intersection time. Therefore, if a unit slope on the derivative plot due to a no-flow boundary condition is available, one should use either Eq. 12 (Whittle and Gringarten, 2008) or Eq. 13, particularly with noise derivatives. If a unit slope on the derivative plot is not available, one should use Eq. 14 with the best possible start time of the observable boundary effect.

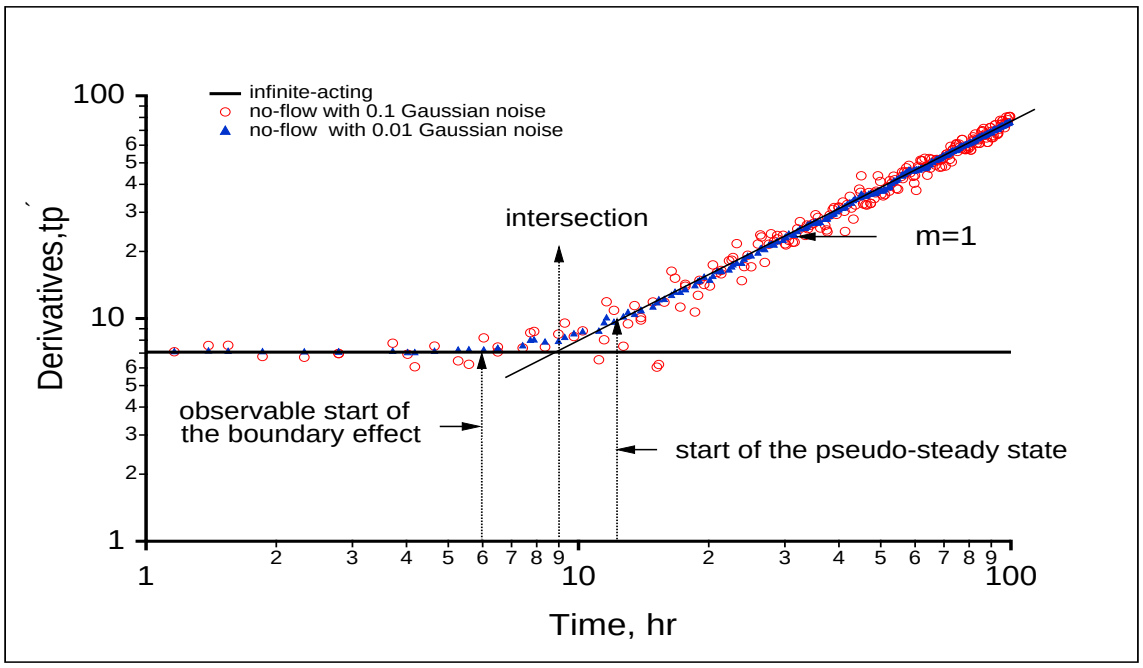


**Fig. 9—Derivatives of the wellbore pressures with noise for an infinite-acting system and a no-flow outer boundary system.**

All of the previous radii of investigation formulae are independent of production rate, thickness of the formation, and pressure-gauge resolution. Furthermore, they are based on the start of the observable boundary effects or pseudosteady-state flow regime. Next, we will present a radius of investigation formula for infinite-acting radial reservoirs, including production rate, thickness of the formation, and pressure-gauge resolution effect. For a line-source well, the pressure distribution in the system can be written as

$$\Delta p(r,t) = \beta_1 \frac{1}{2} \mathrm{E}_1 \left( \beta_2 \frac{r^2}{t} \right), \tag{15}$$

where

$$\begin{aligned} \beta_1 &= \frac{141.2 q \mu}{kh} \\ \beta_2 &= \frac{948.0470}{\eta} \\ \eta &= \frac{k}{\phi \mu c_t}. \end{aligned} \tag{16}$$

Notice that the space-time parameter, $\frac{t}{r^2}$, in Eq. 15 appears as a single variable and is not separable. On the other hand, in the impulse response of the system given as,

$$\Delta p(r,t) = \beta_1 \frac{1}{2t} \exp\left(-\beta_2 \frac{r^2}{t}\right), \tag{17}$$

time $t$ appears also as a separate variable (in Eq. 17). If we were to have a pressure gauge at a distance $r_o$, we would only start to detect a pressure change above the pressure gauge or apparent resolution at $t_o$ with an ideal impulse given by Eq. 17. Let this detectable (observable) pressure change $\Delta p(r_o, t_o)$ be the apparent resolution $\delta p$ in Eq. 17. Solving Eq. 17 for $r_0 = r_{inv}$ (radius of investigation) at $t_0 = t$ yields,

$$r_{inv} = 2\sqrt{\frac{0.0002637kt}{\phi\mu c_t}}\sqrt{\ln\left(\frac{70.6q\mu}{\delta pkht}\right)} = 0.03248\sqrt{\frac{kt}{\phi\mu c_t}}\sqrt{\ln\left(\frac{70.6q\mu}{\delta pkht}\right)}. \tag{18}$$

This equation should not be used for any semi-infinite and bounded systems when the pressure and its derivative of the system deviate from the infinite-acting behavior.

If we run a well test just for 5.4 hr (the observable separation time of the deviation of constant-pressure outer boundary case from the infinite-acting line as shown in Fig. 7), the radius of investigation from the conventional formula given by Eq. 1 is estimated to be 475 ft, 699 ft from Eq. 14, and 856 ft from Eq. 18. If we calculate the pressure drop at these radii at 5.4 hr from Eq. 15, we obtain 2.2 psi at 475 ft, 0.51 psi at 699 ft, 0.16 psi at 856 ft, and 0.10 psi (the resolution we specified in Eq. 18) at 910 ft.

In the previous interference test example (see Fig. 2), the pressure at the observation well was observable above 0.01 psi (the maximum apparent resolution); therefore, all of the previous radius of investigation formulae yield very conservative numbers, except Eq. 18. For example, the radius of investigation computed from the conventional formula given by Eq. 1 is 47% less than the actual value of 910 ft and the estimated reserve from this radius of investigation will be 72% less. The radius of investigation computed from Eq. 18 with a 0.01− psi apparent resolution) is 1, 178 ft.

As discussed earlier, the fundamental problem in determining radius of investigation is that that there is no radius of investigation from the pressure diffusion. The real question is when does a pressure disturbance become observably at a given space? This is basically a function of gauge resolution and natural background noise. In a producing well, drawdown pressures could be noisy, and the noise level could be 10 or hundred times of the gauge resolution. On the other hand, after the initial period of fluid segregation, etc., buildup pressures tend to be measurable at an apparent gauge resolution (pressure gauge resolution plus the background noise).

Figure 10 presents a field drawdown test and a subsequent buildup test. This was a producing well, but it was shut-in for about 20 minutes to allow for lowering production tool into the well. Although the production period was about 6 hr, but due to a production profiling at two different flow rates, the flowing wellbore pressure was not measured at a stationary point until 30 minutes before the start of the buildup. The last wellbore drawdown pressure just before the buildup was 240 psi lower than the pressure at the end of 3 hr production as can be seen in Fig. 10. Both drawdown and buildup pressure data look very smooth except for the initial hump in the drawdown pressure as can as can be seen in Fig. 10. Figure 11 presents a time period toward the end of both tests at the same pressure scales (1 psi for the full scale). As shown in Figure 11, the spread of pressure data in this time frame is about 0.15 psi for drawdown and 0.035 psi for the buildup. Both numbers are greater that the stated 0.01 psi gauge resolution. On the other hand, even for drawdown tests, it is not difficult to reach a 0.1 psi apparent resolution as shown in Fig. 11. For buildup and interference tests, it is easy to achieve an apparent resolution between 0.01 and 0.05 psi with todays quartz pressure gauges that typically have a resolution range from 0.002 to 0.01 psi.

As previously discussed, the fundamental problem in determining radius of investigation is that that there is no radius of investigation from the pressure diffusion. As pointed out, when does a pressure disturbance become observable in a given spatial coordinate? The answer basically depends on gauge resolution and natural background noise. As discussed in details by Daungkaew et al. (2000), many arbitrary criteria were used for obtaining radius of investigation:

1. Many authors used the time at which a pseudosteady-state pressure distribution is attained in a closed circular system.

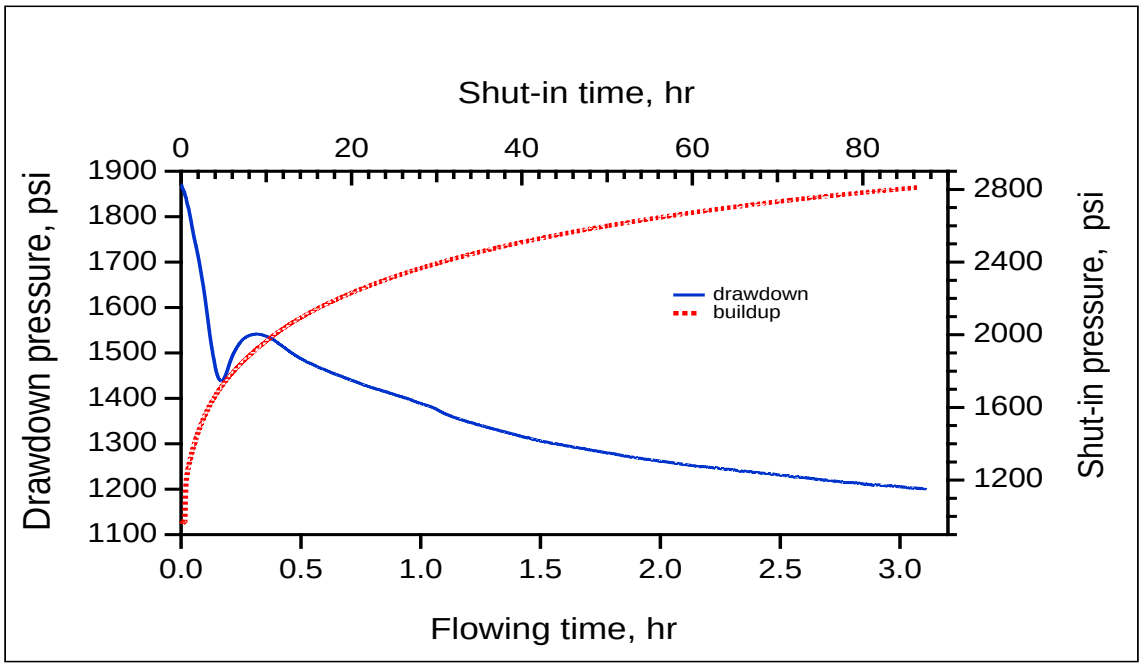


**Fig. 10—Wellbore pressures for a drawdown and a subsequent buildup test.**

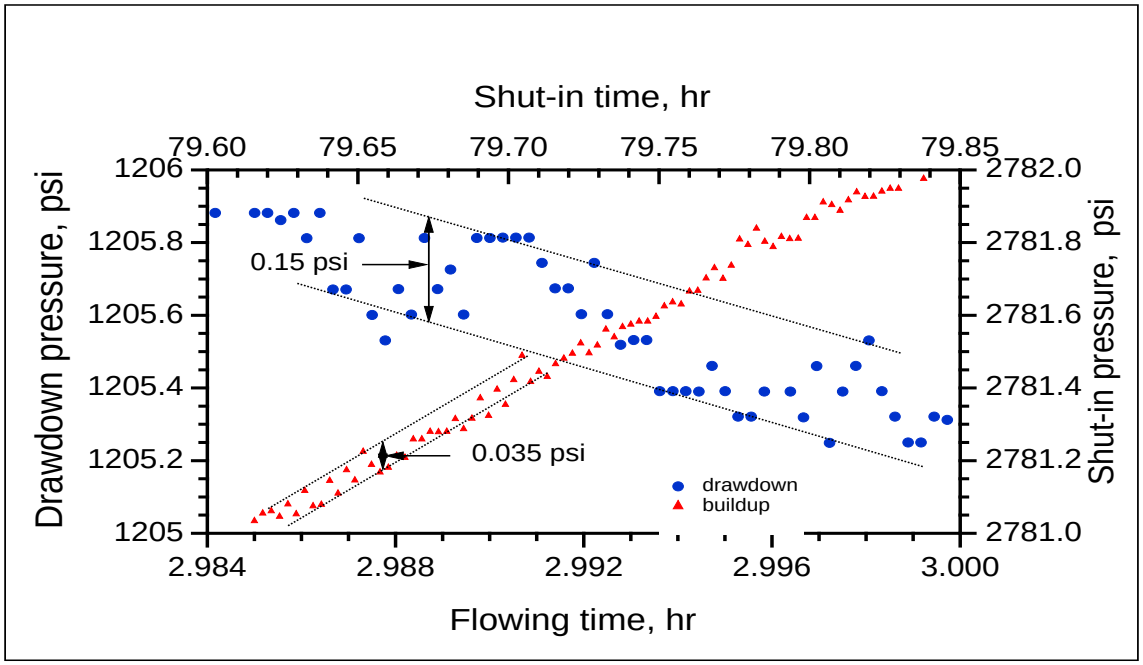


**Fig. 11—A time period showing wellbore pressures for a drawdown and a subsequent buildup test given in Fig 10.**

2. Jones (1962) considered that the radius of drainage is the distance at which the pressure disturbance generated during a drawdown reaches 1% of the pressure drop at the wellbore.

3. citeTeGrPo57 applied a similar approach to Jones (1962) but considered the radius at which the radial flow-rate equals 1% of the flow rate at the wellbore.

4. Muskat (1937) considered the time for the flow regime to reach a pseudosteady-state condition in a bounded reservoir, relatively to the portion of fluid removed from the reservoir.

5. Van Poolen (1964) used the Y function defined by Jones (1962) and the pseudosteady-state condition.

6. Johnson (1988) considered the radius of drainage as being linked to a fraction of the net production during a test.

7. A few authors used the inflection point in the flow rate.

8. Lee (1982) took a radius that makes the impulse response maximum.

9. Hurst (1961) took a radius at which the response of a well in a closed-circular reservoir deviated from the infinite-acting radial flow regime.

10. Finjord (1988) considered a radius taken to be the point at which the flow rate within the formation attained an inflection point based on line source solution.

11. so on.

As we said, there is no a definable radius of investigation from pressure diffusion; therefore, all of these are somewhat arbitrary criteria. An observable pressure change at a given space and time is at least quantifiable above an apparent resolution. Furthermore, it is absolutely quantifiable at the observation wells as shown in Fig. 1. An observable pressure change (a deviation from the infinite-acting behavior) at the wellbore for a given time is also quantifiable at least above an apparent resolution if there is any type of discontinuity such as fractures, faults, constant-pressure and no-flow boundaries in the reservoir. One exception: If the angle between a line from the wellbore to the nearest tip of a sealing-fault and the fault line is close to 180 degrees, its effect is not quantifiable at the producing well. In general, effects of faults and/or fractures are quantifiable at producing and observation wells if their permeabilities are larger than the host formation permeability, provided that the test was run long enough.

In relation radius of investigation, the following obvious observations can be made:

- Transient pressure diffusion in infinite radial-cylindrical media subject to Dirichlet, Neumann, and Robin inner boundary conditions never reaches a pseudosteady state or steady-state condition; *i.e.*, the transient condition of infinite cylindrical systems never ceases (dies).

- The pressure increases logarithmically at a given point when the space-time parameter satisfies the inequality $\frac{t}{r^2} > \frac{4\times10^5}{\eta}$.

- The pressure change will still be significant beyond the logarithmic approximation when the space-time parameter $\frac{t}{r^2} < \frac{4\times10^5}{\eta}$ because the argument $(\frac{\phi\mu c_t r^2}{4kt})$ the exponential integral given in Eq. 15 will not be sufficiently small to approximate the exponential integral by a series expansion (logarithmic approximation). Thus, the logarithmic approximation cannot be used for estimation of the radius of investigation.

The above radii of investigation formulae are given for a single-layer homogenous radial-cylindrical infinite reservoirs for a constant-rate inner boundary condition. As we know, most reservoirs are much more complicated and the flow rate is seldom constant at the sandface. For instance, in any well test, we start with storage effects, Furthermore, most tight formations it is very difficult to maintain the constant flow rate conditions.

**Variable Rate, Skin, and Wellbore Storage**

For convenience, let us assume that a well is produced at a rate of $q_{sf}$ (sandface flow rate) that varies as a function of time. Thus, the pressure change at any time and spatial location in the system can be written from the convolution equation as

$$\Delta p(r,t) = \int_0^t q_{sf}(\tau) g(r, t-\tau) d\tau, \tag{19}$$

where $\Delta p = p_o - p$, $g$ is the impulse response of a single-phase system (fractured, layered, homogenous, heterogeneous, etc.), where Darcy's law is valid and $q_{sf}$ is the sandface flow rate. In the Laplace domain, Eq. 19 becomes

$$\Delta \bar{p}(r,s) = \bar{q}_{sf}(s) \bar{g}(r,s), \tag{20}$$

where $s$ is the Laplace domain variable. If the compressibility of the fluid in the production string remains constant during annulus unloading, then the wellbore (sandface) flow rate can be expressed as

$$q_{sf}(t) = q_m(t) + C \frac{dp_w}{dt}, \tag{21}$$

where $q_m$ is the measured flow rate at any location in the wellbore including the wellhead and sandface, and $C$ is the wellbore storage coefficient is given as $C = c_w V_w$, where $c_w$ is the compressibility of the wellbore fluid and $V_w$ is the wellbore volume below the measuring point. Note that in general neither the sandface flow rate $q_{sf}$ nor the measured flow rate $q_m$ need be constant. Eq. 21 is to be solved in conjunction with the well response and the initial condition given as

$$p_w = p_o \quad \text{at } t = 0, \tag{22}$$

Therefore, Eq. 21 in the Laplace domain becomes

$$\bar{q}_{sf}(s) = \bar{q}_m(s) + C \left[ s \bar{p}_w(s) - p_o \right], \tag{23}$$

where $p_w$ is the wellbore pressure that can be written as

$$\bar{p}_w(r_w, s) = \frac{p_o}{s} - \frac{\bar{q}_m(s) \bar{g}_w(r_w, s)}{1 + Cs \bar{g}_w(r_w, s)}, \tag{24}$$

where the wellbore impulse response $g_w = g_f + \Delta p_{skin}$, $g_f$ is the impulse response due to the formation in the wellbore, and $\Delta p_{skin}$ is the pressure drop due to skin $S$. Substitution of Eq. 24 in Eq. 23 yields

$$\bar{q}_{sf}(s) = \frac{\bar{q}_m(s)}{1 + Cs \bar{g}_w(r_w, s)}. \tag{25}$$

Substitution of Eq. 25 in Eq. 20 gives the pressure change at any time and spatial location in the system as

$$\Delta \bar{p}(r,s) = \left[ \frac{\bar{q}_m(s)}{1 + Cs \bar{g}_w(r_w, s)} \right] \bar{g}(r,s) \tag{26}$$

.

If $q_m$ the measured flow rate is constant at the surface, the above equation becomes

$$\Delta \bar{p}(r,s) = \frac{q}{[1 + Cs \bar{g}_w(r_w, s)]} \frac{\bar{g}(r,s)}{s} \tag{27}$$

.

Normally one should determine the radius of investigation after the effect of the wellbore storage diminishes. As can be seen from Eqs. 26 and 27, when the producing time becomes large as $s \to 0$, $\Delta \bar{p}(r,s)$ becomes $\frac{\bar{g}(r,s)}{s}$ which is not a function of the wellbore storage.

Figure 12 presents effects of wellbore storage and skin on the pressure distribution in the reservoir for parameters are given in Table 2 with a production rates, $q$, 1,000 B/D, $t_p$=1 hr, $C_D$=10,000, and $S$=20. It should be pointed out that we took a small producing time $t_p$ just to show the effects of wellbore storage and skin. The same figure

also presents the pressure distribution for the infinite-acting case without storage and skin. For instance, the radii of investigation will be 250 ft if an apparent resolution is 0.01 psi with the wellbore storage and skin effects and about 500 ft without storage and skin. It will be 588 ft from Eq. 18. Therefore, in general, it will be much more accurate if the radius of investigation is directly determined, as shown in Fig. 12, from the reservoir model. In other words, after the system identification, the parameter estimation, and validation steps of interpretation, one should graphically determine, as shown in Fig. 12, the radius, area, or volume of investigation from the reservoir model.

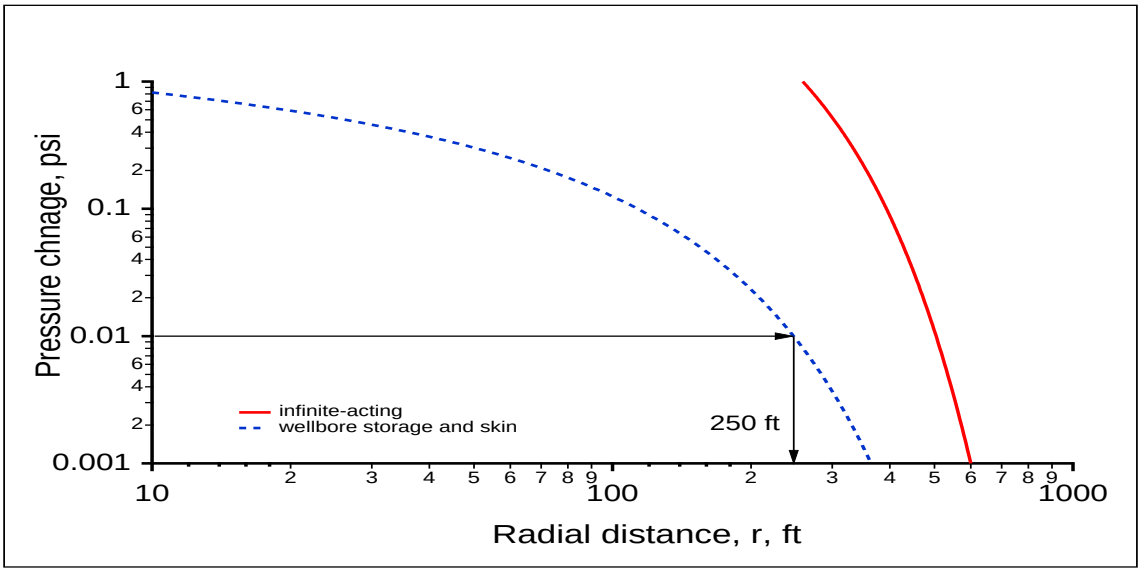


**Fig. 12—Reservoir pressure distribution with and without wellbore storage and skin effects.**

To show the effect of flow rate variations, we will consider two different cases (Kuchuk, 1990; Streltsova, 1988):

1. A linear production rate decline (**Case 1**) after the start of the drawdown can be described as

$$q_{sfD}(t_D) = 1 - \alpha t_D, \tag{28}$$

where $q_{sfD} = q_{sf}/q$ is a normalized rate, $q_{sf}$ is sandface flow rate, $q$ is the reference flow rate, and $\alpha$ is a positive constant. The decline of the production rate after the start of the drawdown is very common in low permeability reservoirs, particularly fractured wells. It also occurs if the permeability of the formation is pressure sensitive.

2. A linear production rate increase (**Case 2**) after the start of the drawdown can be described as

$$q_{sfD}(t_D) = \alpha t_D, \tag{29}$$

The production increase could usually occur when wellbore storage and skin are large, a well or a hydraulic fracture is still cleaning up.

In both cases we have chosen a value of $\alpha$ so that the cumulative production will be identical for both cases. In other words, $q_{sfD}$ will be 1 at the end of the production period for the increasing rate case and $q_{sfD}$ will be 0 at the end of the production period for the decreasing rate case.

The pressure distribution in the system for a line-source well (Eq. 15) for **Case 1** (the linear production rate decline) can be written from Eq. 20 in Laplace domain as

$$\bar{p}_D(r_D, s_D) = \left(\frac{1}{s_D} - \frac{\alpha}{s_D^2}\right) \mathrm{K}_0\left(\mathrm{r_D}\sqrt{\mathrm{s_D}}\right), \tag{30}$$

where $s_D$ is the Laplace domain variable, and in the time domain (Kuchuk, 1990; Streltsova, 1988)

$$p_D(r_D,t_D)=\frac{1}{2}\,\mathrm{E}_1\left(\frac{r_D^2}{4t_D}\right)\left[1-\alpha\left(t_D+\frac{r_D^2}{4}\right)\right]+\alpha t_D\exp\left(-\frac{r_D^2}{4t_D}\right). \tag{31}$$

Similarly, for the linear production rate increase (**Case 2**) the pressure distribution in the system can be written as

$$\bar{p}_D(r_D,s_D)=\frac{\alpha}{s_D^2}\mathrm{K}_0\left(\mathrm{r_D}\sqrt{\mathrm{s_D}}\right) \tag{32}$$

and in the time domain (Kuchuk, 1990; Streltsova, 1988)

$$p_D(r_D,t_D)=\frac{\alpha}{2}\,\mathrm{E}_1\left(\frac{r_D^2}{4t_D}\right)\left(t_D+\frac{r_D^2}{4}\right)-\alpha t_D\exp\left(-\frac{r_D^2}{4t_D}\right). \tag{33}$$

A simple examination of Eqs. 31 and 33 indicates that for a small $\alpha<1$ the pressure change in any location of the system will be small for the linear production rate increase (**Case 2**) when it is compared with **Case1** for the same cumulative production. Figure 13 presents the pressure distributions in the reservoir for parameters are given in Table 2 with a production rates, $q=1,000\,\mathrm{B/D}$, $t_p$= 10 hr, and $\alpha=0.00000092$ (dimensionless) for **Case 1**, **Case 2**, and the constant-rate case. For instance, the radii of investigation will be 1580 ft for **Case 1** and 1330 ft for **Case 2** if an apparent resolution is 0.01 psi. It is interesting to note that the radius investigation for **Case 1** is almost same as the constant-rate case. On the other hand, the cumulative production for **Case 1** is half of the constant-rate case cumulative production. Therefore, if we have to produced a limited amount in a DST or a production test, it is much better to start at very high rate and reduce with time to attain a maximum radius of investigation for a given produced volume, provided that the rate is measured.

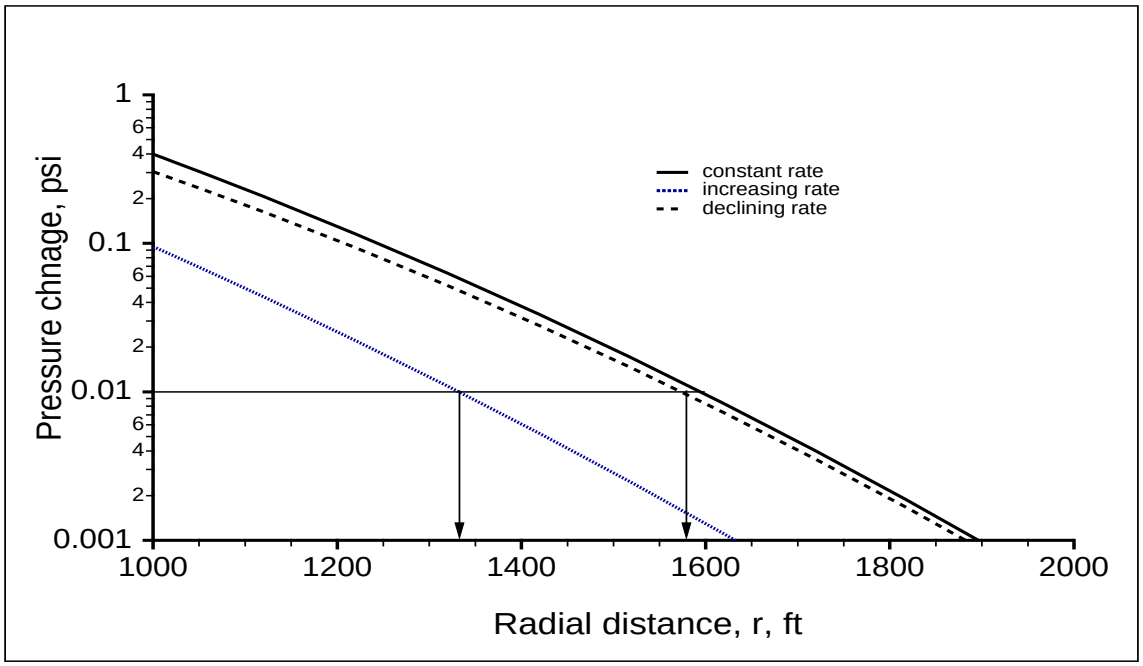


**Fig. 13—Reservoir pressure distributions for linearly declining and increasing flow rate cases.**

## Generalized Radius of Investigation

In recent years, various investigators (Boutaud de la Combe et al., 2005; Kuifu, 2007, 2008; Larsen and Straub, 2007; Levitan et al., 2006) presented several techniques for calculating the radius of investigation from the best-fit reservoir

models. Kuifu (2007) and Kuifu (2008) in both papers have used shrinking box approach. For the model base radius of investigation calculations, simple we should obtain a radius at which the pressure change should be above or equal to the apparent resolution. Furthermore, one should be very careful if the numerical models are used for obtaining radius of investigation because the grid-block size becomes very large away from the wellbore and the solution may not have a good accuracy away from the wellbore.

We have already discussed in the Variable Rate and Skin and Wellbore Storage section how to determine a model based the radius investigation. Next, we will present another example for a model based radius of investigation determination. Suppose that after a pressure transient well test interpretation, the final reservoir model is homogeneous reservoir with a sealing fault as given by Eq. 7. Further assume that the parameters obtained from the interpretation are given in Table 2 with $r_w$= 0.35 ft, $d$ = 700 ft, and production rate, $q$ = 1,000 B/D. The distance to the fault should also be determined from the well test interpretation. The derivative plots, etc. are given above for this example.

Figure 14 presents a contour plot of the pressure distribution in the reservoir with a fault at $t_p$= 10 hr. As can be seen from this figure, after the effect of the boundary, the pressure distribution is not symmetric about the origin anymore. The equipressure contours are not concentric circles, but they are distorted circles. At $t_p$= 10 hr, if we want to determine reserve, we have to take a contour at the apparent gauge resolution to obtain an observable area of investigation. It should be pointed out that the area between 0.1 and 0.01 psi contours are quite large. Of course, this will have a significant effect on the estimated reserve. Therefore, it is very important to use a very accurate apparent resolution for determining a radius, area, or volume of investigation. with the reservoir model.

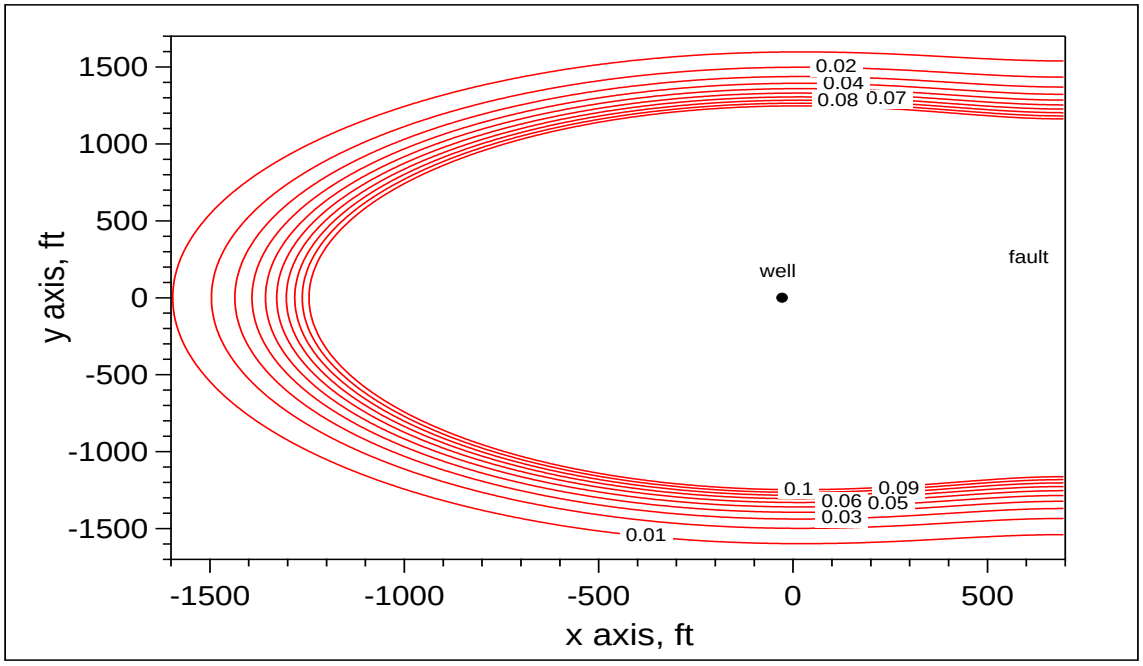


**Fig. 14—Pressure distribution in the reservoir for the sealing fault example.**

## Apparent Resolution

In addition to the final reservoir model obtained from a pressure transient well test and geoscience data, we need an apparent resolution to determine a model based radius investigation or from Eq. 18. The minimum apparent resolution is the gauge resolution that is normally stated by manufacturers (service companies, vendors, etc); the gauge resolution is the minimum pressure change that can be detected by the sensor. However, many parameters affect the gauge resolution and over all performance of the downhole system including the downhole gauge electronics and packaging. Particularly, the drift with time should be minimum.

Before any well test, the pressure gauge should be calibrated and uncertainty in resolution, drift, accuracy, etc should be established. Other factors like thermal effects should be determined. When the data are acquired, the stable part of the drawdown, the last portion of buildup, or the initial part of an interference test should be plotted at the gauge resolution scale as shown Fig. 2 and Fig. 11. Let us re-plot the test given by Figure 2 as shown Fig. 15 and determine the standard deviation $\sigma$ of the pressure measurements for a stable $1-$ hr period. As shown in the figure, $\sigma$ =0.00183 psi. Thus, the apparent resolution for this test is $2\sigma$ =0.00366 psi. If we want to be conservative, then $\sigma_{max}$ =0.0103 psi as shown in the figure should be used as the apparent resolution.

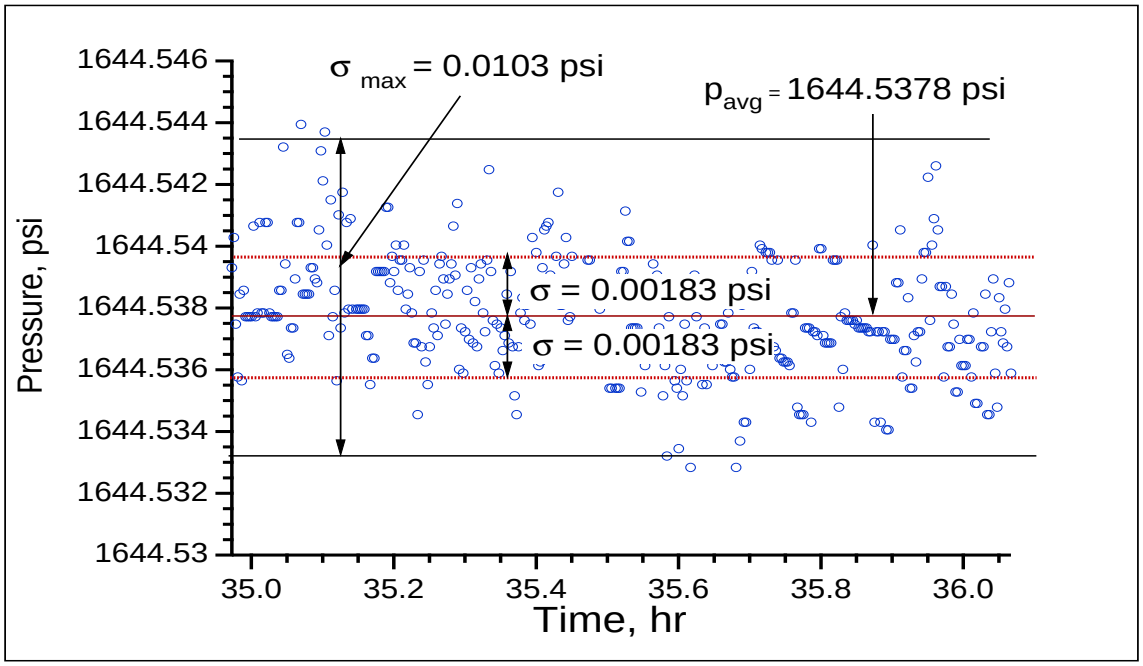


**Fig. 15—Determination of an apparent resolution from an interference test data.**

## Summary and Conclusions

In this paper, we have investigated the radius of investigation concept from pressure diffusion. There is only one definable radius of investigation for fluid flow in porous media that comes from the pressure propagation and not from the pressure diffusion. Furthermore, there is no identifiable radius of investigation from the pressure diffusion. We have shown that many different arbitrary criteria have been used to define a radius of investigation from the pressure diffusion. We have presented a new formula for observable radius of investigation in radial-cylindrical infinite systems. This new formula takes into account the production rate, formation thickness, and gauge resolution. It has been shown that the conventional radius of investigation formula for radial-cylindrical systems, which is given as $r_{inv} = 0.029\sqrt{\frac{kt}{\phi\mu c_t}}$, yields very conservative estimates; it could be 40% lower, which could yield a 60% lower reservoir volume estimate. Observable radius of investigation is fundamental to understanding how much reservoir volume is being investigated for a given duration of a transient test. Finally, radius, area, or volume of investigation should be obtained from the final reservoir model after the well test interpretation with geoscience data and an apparent resolution.

## Nomenclature

$A$ = area
$c$ = compressibility or constant
$C$ = wellbore storage constant

$d$ = distance
$\mathrm{E}_1$ = The exponential integral
$g$ = impulse response
$h$ = formation thickness
I = modified Bessel Function of the first kind
K = modified Bessel Function of the second kind
$k$ = permeability
$p$ = pressure
$q$ = flow rate
$r$ = radius or radial coordinate
$S$ = skin
$s$ = Laplace transform variable
$t$ = time
$v$ = velocity
$V$ = volume
$x$ = coordinate
$y$ = coordinate
$z$ = vertical coordinate
$\alpha$ = constant
$\beta$ = constant
$\eta$ = diffusivity for pressure
$\mu$ = viscosity
$\phi$ = porosity
$\sigma$ = standard deviation
$\tau$ = dummy variable
Subscripts
$D$ = dimensionless
$e$ = external boundary
$f$ = formation
$h$ = horizontal
$m$ = measured
$o$ = initial or original
$sf$ = sandface
$r$ = radius
$t$ = total
$w$ = wellbore
Subscripts

**Acknowledgments**
The author is grateful to Schlumberger for permission to present this paper and would like to thank Dr. Mustafa Onur of Technical University of Istanbul for valuable discussions.

## References

Boutaud de la Combe, J., O. Akinwumni, C. Dumay, and M. Tachon (2005). Use of DST for effective dynamic appraisal : Case studies from deep offshore West Africa and associated methodology. SPE 97113, SPE Annual Technical Conference and Exhibition, Dallas, Texas.

Brownscombe, R. and L. Kern (1951). Graphical solution of single- phase flow problems. *The petroleum engineer*, B–70.

Chatas, A. (1953). A practical treatment of nonsteady-state flow problems in reservoir systems. *The petroleum engineer*, B–44.

Daungkaew, S., F. Hollaender, and A. Gringarten (2000). Frequently asked questions in well test analysis. SPE 63077, SPE Annual Technical Conference and Exhibition, Dallas, Texas.

Earlougher, R. (1977). *Advances in Well Test Analysis* (First ed.). Monograph Series 5. Dallas, TX: Society of Petroleum Engineers of AIME.

Finjord, J. (1988). Discussion of the relationship between radius of drainage and cumulative production. *SPE Formation Evaluation Journal*, 670.

Foster, W., J. McMillen, and A. Odeh (1967). The equations of motion of fluids in porous media: I. propagation velocity of pressure pulses. *SPE Journal*, 333–341.

Horner, D. (1951). Pressure buildup in wells. In E. J. Brill (Ed.), *Proceedings*, Leiden. Third World Petroleum Congress.

Hurst, W. (1934). Unsteady flow of fluids in oil reservoirs. *Journal of Applied Physics* (5), 20–30.

Hurst, W. (1961). Some problems in pressure build-up. *The Oil And Gas Journal*, 66–69.

Hurst, W., O. Haynie, and R. Walker (1969). The radius of drainage formula. SPE 145, SPE Annual Fall Meeting of the Society of Petroleum Engineers, Dallas, Texas.

Johnson, P. (1988). The relationship between radius of drainage and cumulative production. *SPE Formation Evaluation Journal*, 267–270.

Jones, P. (1962). Reservoir limit test on gas wells. *Journal of Petroleum Technology*, 613–618.

Kuchuk, F. (1990). Gladfelter deconvolution. *SPEFE*, 285–292.

Kuifu, D. (2007). Use of advanced pressure transient analysis techniques to improve drainage area calculations and reservoir characterisation: Field case studies. SPE 109053, Offshore Europe, Aberdeen, Scotland.

Kuifu, D. (2008). The determination of tested drainage area and reservoir characterization from entire well-test history by deconvolution and conventional pressure-transient analysis techniques. SPE 116575, SPE Annual Technical Conference and Exhibition, Denver, Colorado.

Kutasov, I. and S. Hejri (1984). Drainage radius of a well produced at constant bottomhole pressure in an infinite acting reservoir. Unsolicited SPE 13382, Society of Petroleum Engineers, Dallas, Texas.

Larsen, L. and R. Straub (2007). Determination of connected volume and connectivity from extended tests in compartmentalised and layered reservoirs. SPE 110011, SPE Annual Technical Conference and Exhibition, Anaheim, CA.

Lee, W. (1982). *Well Testing*. Dallas, Texas: Society of Petroleum Engineers.

Levitan, M., M. Ward, J. Boutaud de la Combe, and M. Wilson (2006). The use of well testing for evaluation of connected reservoir volume. SPE 102483, SPE Annual Technical Conference and Exhibition, San Antonio, Texas.

Miller, C., A. Dyes, and H. C.A.Jr. (1950). The estimation of permeability and reservoir pressure from bottom-hole pressure buildup characteristics. *Trans., AIME 189*, 91–104.

Morse, P. and H. Feshback (1953). *Methods of Theoretical Physics*. New York: McGraw-Hill.

Muskat, M. (1934). The flow of compressible fluids through porous media and some problem in heat conduction. *Physics 5*(71).

Muskat, M. (1937). *The Flow of Homogeneous Fluids Through Porous Media*. Ann Arbor, Michigan: J. W. Edwards, Inc.

Ramey, H. and W. M. Cobb (1971). A general pressure buildup theory for a well in a closed drainage area. *Journal of Petroleum Technology*.

Stewart, G. (2007). Depth of investigation and relation to gauge resolution. A presentation at SPE ATW on Reservoir Testing in a World of High Production Values, Bali, Indonesia.

Streltsova, T. (1988). *Well Testing in Heterogeneous Formations* (First ed.). New York: John Wiley & Sons.

Tek, M., M. Grove, and F. Poettmann (1957). Method for predicting the back-pressure behavior of low-permeability natural gas-wells. *Trans. AIME*, 210–302.

van Everdingen, A. and W. Hurst (1949). The application of the laplace transformation to flow problems in reservoirs. *Trans., AIME 186*, 305–324.

Van Poolen, H. (1964). Radius-of-drainage and stabilization-time equations. *The Oil and Gas Journal*, 138–146.

Whittle, T. and A. Gringarten (2008). The determination of minimum tested volume from the deconvolution of well test pressure transients. SPE 116575, SPE Annual Technical Conference and Exhibition, Denver, Colorado.